объединенный
институт
ядерных
исследований
дубна

E13-92-545

FASA — A 4π DETECTOR SETUP FOR THE INVESTIGATION OF TARGET MULTIFRAGMENTATION IN NUCLEUS-NUCLEUS COLLISIONS

Submitted to «Nuclear Instruments and Methods»

1992

Авдеев С.П. и др. E13-92-545

ФАЗА-4π — установка для исследования мультифрагментации мишени в ядро-ядерных соударениях

Установка ФАЗА размещена на пучке синхрофазотрона ОИЯИ, ускоряющем легкие ядра до энергии 3,65 ГэВ/нуклон. Это детектор множественности фрагментов, состоящий из 55 сцинтилляционных счетчиков с пленочными CsJ(Tl), пяти время-пролетных телескопов и позиционно-чувствительной плоско-параллельной лавинной камеры большой площади. Время-пролетные телескопы позволяют определять с высокой точностью энергию, массу и скорость детектируемых фрагментов, в то время как сцинтилляционные счетчики дают информацию о полной множественности фрагментов в событии. Триггерами системы являются телескопы. Установка позволяет также измерять угловые корреляции и распределения, а также корреляции по относительной скорости для совпадающих фрагментов.

Работа выполнена в Лаборатории ядерных проблем ОИЯИ.

Препринт Объединенного института ядерных исследований. Дубна 1992

Avdeyev S.P. et al. E13-92-545

FASA - a 4π Detector Setup for the Investigation of Target Multifragmentation in Nucleus-Nucleus Collisions

The FASA setup, installed at the JINR synchrophasotron providing light ion beams with energies up to 3.65 GeV/nucleon, is a fragment multiplicity detector, consisting of 55 scintillation counters made of thin CsI(Tl) films, five time-of-flight telescopes and a large area position-sensitive parallel-plate avalanche chamber. The basic aim of the device is to determine with high precision the energy, mass and velocity of the fragments detected in the time-of-flight telescopes (TOF) while for the other fragments global multiplicity information is obtained. Therefore, the TOF telecopes serve as a trigger. In addition, angular correlations and distribution and relative velocity correlations for coincident fragments can be measured with the FASA setup.

The investigation has been performed at the Laboratory of Nuclear Problems, JINR.

Preprint of the Joint Institute for Nuclear Research. Dubna 1992

S.P.Avdeyev, V.A.Karnaukhov, W.D.Kuznetsov, L.A.Petrov
Joint Institute for Nuclear Research, Dubna, Head Post Office, P.O.Box 79,
Moscow, Russia

R.Barth, V.Lips, H.Oeschler
Institut für Kernphysik, Technische Hochschule Darmstadt,
D-6100 Darmstadt, Germany

O.V.Bochkarev, L.V.Chulkov, E.A.Kuzmin, I.G.Mukha, V.A.Olkin,
G.B.Yankov
Kurchatov Institute, P.O.Box 123182, Moscow, Russia

W.Karcz
Henryk Niewodniczanski Institute of Nuclear Physics, 31-342 Cracow, Poland

Y.T.Vidaj
Monocrystal Institute, P.O.Box 310141, Kharkov, Ukraine

W.Neubert
Institut für Kern- und Hadronenphysik, Forschungszentrum Rossendorf,
D-8051 Dresden, Germany

E.Norbeck
University of Iowa, Iowa City, IA 52242, USA

1 Introduction

The process of multiple emission of intermediate mass fragments (IMF) from a highly excited nuclear system has been the subject of intensive studies in recent years. There are two reasons for that. Firstly, multifragment emission is known to be an important decay mode of hot nuclear systems whereas the mechanism governing this process is not yet fully understood. Secondly, the investigation of the multifragment process should give information on the possibility of the liquid-gasphase transition in the nuclear media and hence basic knowledge of nuclear matter properties.

A great amount of inclusive experimental data on this topic has been collected up to now, but detailed information on the mechanism and the time scale of this process can only be gained by the use of multidetector, 4π systems. Presently, several 4π-setups for fragment detection are in operation or under construction (for a recent review see ref. [1]).

In this paper we describe the FASA device, which is designed to study target multifragmentation induced by light ions, accelerated by the JINR synchrophasotron to energies up to 3.65 GeV/nucleon.

The basic concept of the device stems from the fact that for most studies it is sufficient to measure the properties of a few fragments with high precision while for the 4π coverage only global information is needed. Very important information is expected from the studies of the relative velocity and angular correlations of coincident fragments.

2 The FASA setup

The general view of FASA is shown in fig. 1. The main body of the device is a welded steel frame with the shape of a dodecahedron, ten sides of which carry steel flanges with six counters. Two flanges centered on the beam axis are connected with the entry and exit pipes of 200 mm diameter. These flanges have only five counters. The entry and exit pipes rest on the bearings of semicircular supports fixed at the top of steel pillars. The device can be rotated around the horizontal axis and fixed as necessary for comfortable mounting.

The polyhedron formed by the front faces of the detectors is shown in fig. 2. It consists of 12 regular pentagons (marked black), surrounded by 60 irregular hexagons. This polyhedron may be thought to originate from the Archimedean pentagonal hexecontahedron, consisting of 60 irregular pentagons, by cutting 12 five-fold vertices by regular pentagons [2]. The cut-off line is chosen to make the solid angles of all detectors equal. Each pentagonal detector is located directly opposite another pentagonal detector.

The device consists of a fragment-multiplicity-detector array (FMD), five time-of-flight telescopes (TOF), serving as a trigger of the system and a large-area position-sensitive parallel-plate avalanche counter (PPAC).

The FMD is composed of 55 scintillation counters using thin CsI(Tl) layers with a thickness of about 20 mg/cm^2 evaporated on a 2 mm plexiglass backing. The scintillation light is transported by conic plexiglass light guides, onto photomultiplier tubes of type FEU-110. The entrance parts of the light guides are shaped to fit to the hexagon or pentagon backing of the CsI(Tl) scintillator. Figure 3 shows one module with five scintillation counters and one TOF telescope in the middle position.

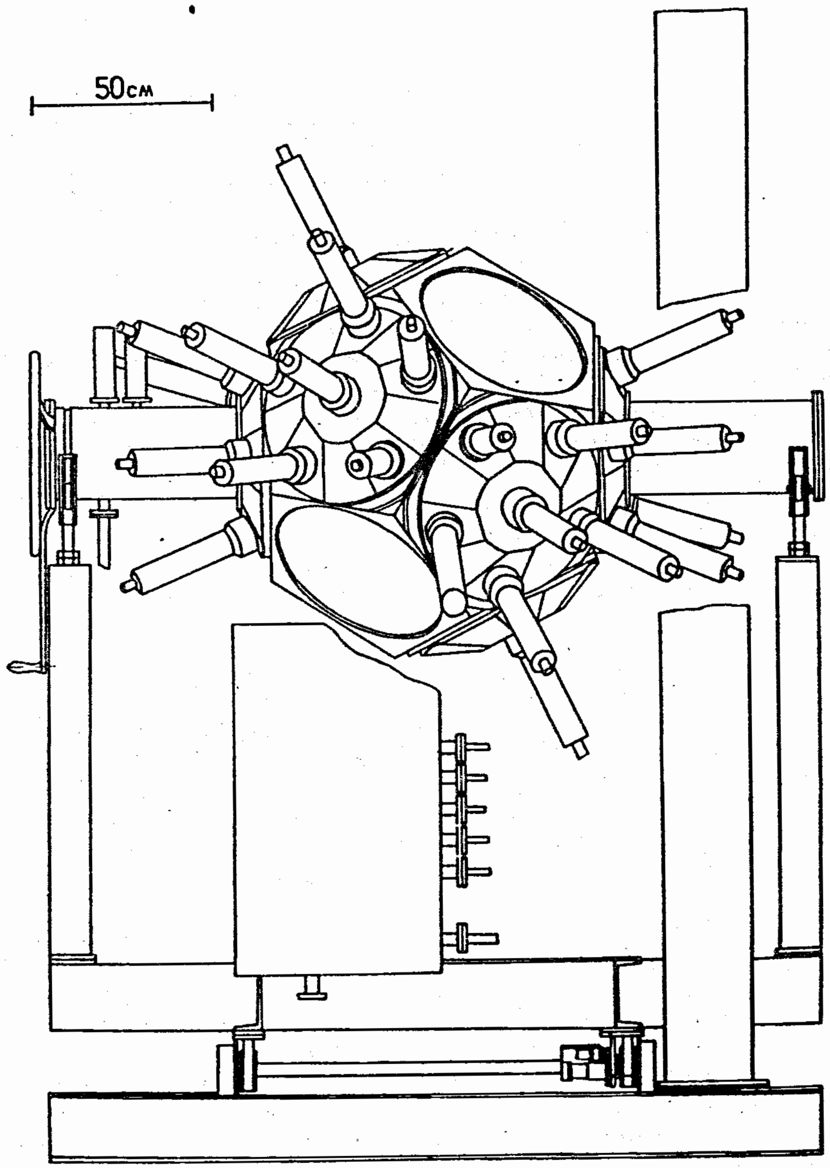

Fig. 1 General view of the FASA setup.

Each of the five TOF telescopes consists of a parallel-plate avalanche counter (AC) as a start detector and a surface-barrier detector (SBD) to give the energy information and a time-stop signal.

One flange carries a position-sensitive parallel-plate avalanche chamber (PPAC) with a size of 30×30 cm^2. Together with the five telescopes this chamber allows the determination of the relative velocity and angular correlations of coincident fragments.

The target is located in the centre of the vacuum chamber. The distance between the midpoints of the target and the scintillation counters is 29 cm. The beam spot has typical half widths of 30 mm in the horizontal and 10 mm in the vertical direction. As targets we used in the first experiments self-supporting gold foils of about 1 mg/cm^2 thickness with dimensions of 60×60 mm^2. The target plane is tilted by 45^0 in respect to the beam axis. In order to minimize the material close to the beam, the target is glued onto two parallel tungsten wires of 26 μm diameter. The target foil is further supported by two 8 μm thick tungsten wires in the middle part. The wires are fixed on an U-shaped frame of plexiglass. The minimal distance between the centre of the beam spot and this frame is 180 mm so that the tails of the beam would not hit the frame.

For the energy calibration of the various detectors an ^{241}Am α-source was used. It was made by electroplating onto the surface of a stainless steel sphere of 10 mm in diameter. During the runs the α-source is removed into a cylindrical housing which is closed automatically by a cap. This housing is located at 30 cm distance from the beam axis. To monitor the amplitude stability of the photomultipliers during the experiments a LED was mounted inside the vacuum chamber. It was operated by a pulser, giving three light flashes per spill.

3 Scintillation counters

3.1 Fabrication of thin scintillators

Thin polycrystalline CsI(Tl) films are prepared by thermal vacuum evaporation according to the technology developed at the Kharkov Institute of Monocrystals [3]. Plexiglass plates of 2 mm thickness are used as a backing. Their shapes are shown in fig. 4. An evaporation procedure had been developed that obtains uniformity in the film thickness of better than 15%. Two boats (18×100 mm^2) at 80 mm distance from each other are used at a distance of 180 mm from the scintillator backing. Each scintillator is produced in two steps with turning the backing by 90^0 around the normal to its surface. As a raw material the crushed monocrystal of CsI(Tl) is used with an activator concentration of 0.8% – 1.2%. One side of the backings is sanded to improve the adhesiveness for the CsI(Tl). The backing is heated up to $40^0 - 50^0$ C during the evaporation to improve the quality of the scintillator film for obtaining good uniformity and better contact. More heating provokes reemission of Tl and a decrease of the activator concentration in the film.

A small plexiglass plate of 20×20 mm^2 is placed at the side of the backing to get a control sample, which is used for the film thickness determination by weighting and for measurements of the scintillation characteristics.

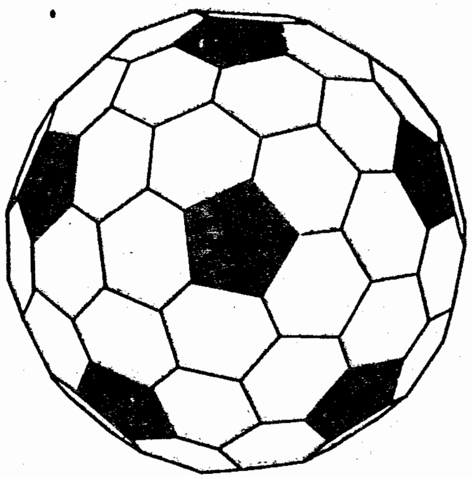

Fig. 2 The polyhedron formed by the front faces of the CsI(Tl) detectors. The pentagons are marked in black, the irregular hexagons in white.

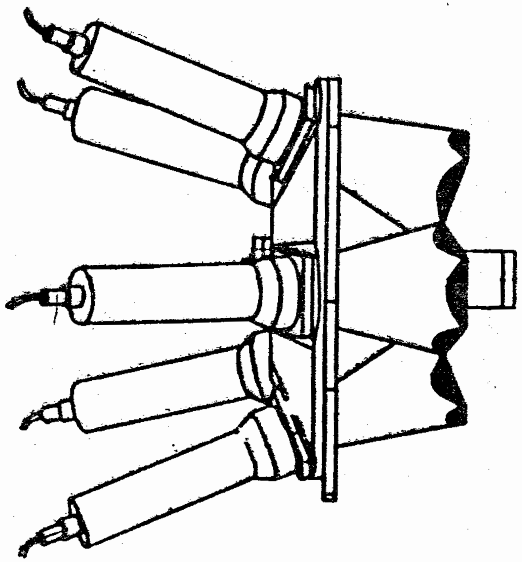

Fig. 3 One of the twelve moduls of FASA consisting of five CsI(Tl) scintillators and one TOF telescope.

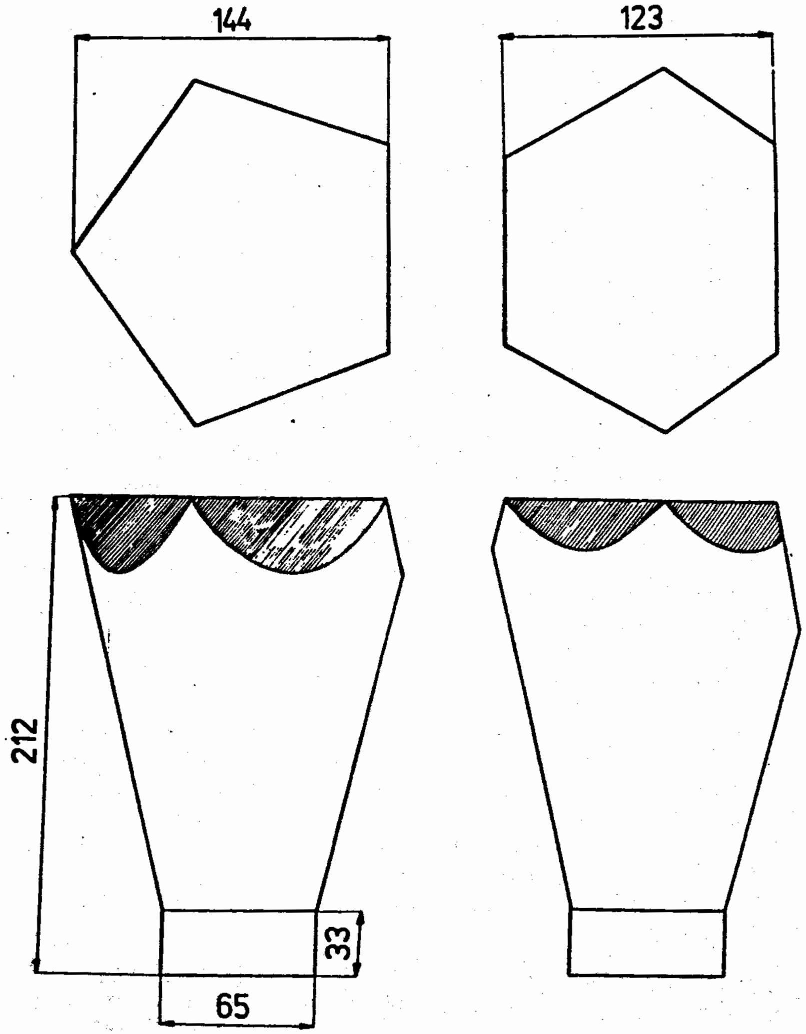

Fig. 4 Front and side view of the light guides, the lengths are given in mm.

3.2 Properties of the scintillator layers measured with α-particles

The energy resolution of the thin CsI(Tl) has been measured using a ThC-α-source (E_α=6.05 MeV and 8.78 MeV). The first measurements were performed with α-particles collimated on a spot of 1 cm^2 in the centre of the scintillator. An example of the spectra is shown in fig. 5A. The light output for polycrystalline CsI(Tl) is approximately the same as for the monocrystalline one, but the amplitude resolution deteriorates from $\approx$10% to $\approx$15%.

The selfabsorption length $\lambda_{1/2}$ of polycrystalline CsI(Tl) was found to be 16–20 mg/cm^2 by comparing the peak amplitude for α-particles going into the film perpendicularly and at a grazing angle. For these measurements a ^{238}Pu-source was used, since the range of the 5.5 MeV α- particles is less than the film thickness. As a consequence it is not reasonable to use films with a thickness significantly larger than 20 mg/cm^2.

The CsI(Tl) detectors described here are intended for the registration of rather slow nuclear fragments with high specific energy losses. Therefore, any significant dead layer on the surface of the scintillators would be very disturbing. Dead layers of 3–5 mg/cm^2 on the surface of polished monocrystalline CsI(Tl) are reported (see for example ref.[4]). A dead layer manifests itself by a cutoff in the dependence of the peak position L as a function of the particle energy E_α. To determine the dead layer an α-source of ^{238}Pu was placed in the vacuum chamber at a distance of 25 cm to the scintillator, covered by a screen with a hole of 20 mm diameter. The pulse height spectra of the α-particles were measured for various energies whereby the energy was changed by alteration of the air pressure in the chamber. As shown in fig. 6 the quantity L/E_α is only slightly changing with the decrease of E_α down to 0.3 MeV which indicates that the dead layer is less than 1 mg/cm^2.

3.3 Light guides

The light guides are made from plexiglass with surfaces polished except for the cuttings on the conical part. To optimize the light transmission on the borders between the light guide and the phototube the silicon oil Baysilon M-1 000 000 is used. Here a good optical contact is of great importance, while putting the optical fluid between the CsI(Tl) backing and the light guides does not increase the signal amplitude. This is caused by the conical shapes of the light guides. The light reflection on the light-guide face is insignificant because the angular acceptance of the light guide does not exceed 50^0. The transmission through the light guide is about 30%.

Furtheron, a possible dependence of the signal amplitude upon the position of the scintillation flash was investigated. The measurements were performed with a remote α-source and different circular masks on the surface of the scintillator. It was found that in a fully polished light guide the signal amplitude increases significantly when the flash position is shifted from a midpoint of the scintillator to its periphery. This effect can be explained by the increase of the angular acceptance caused by the cuttings on the entry part of the light guide. A blackening of these cuttings provides a good compensation for this edge effect. The same result has been obtained by leaving these parts of the light guides unpolished after machining.

The spectrum shown in fig. 5B was obtained for a light guide with black cuttings, the whole surface of the scintillator was irradiated by α-particles from a source placed

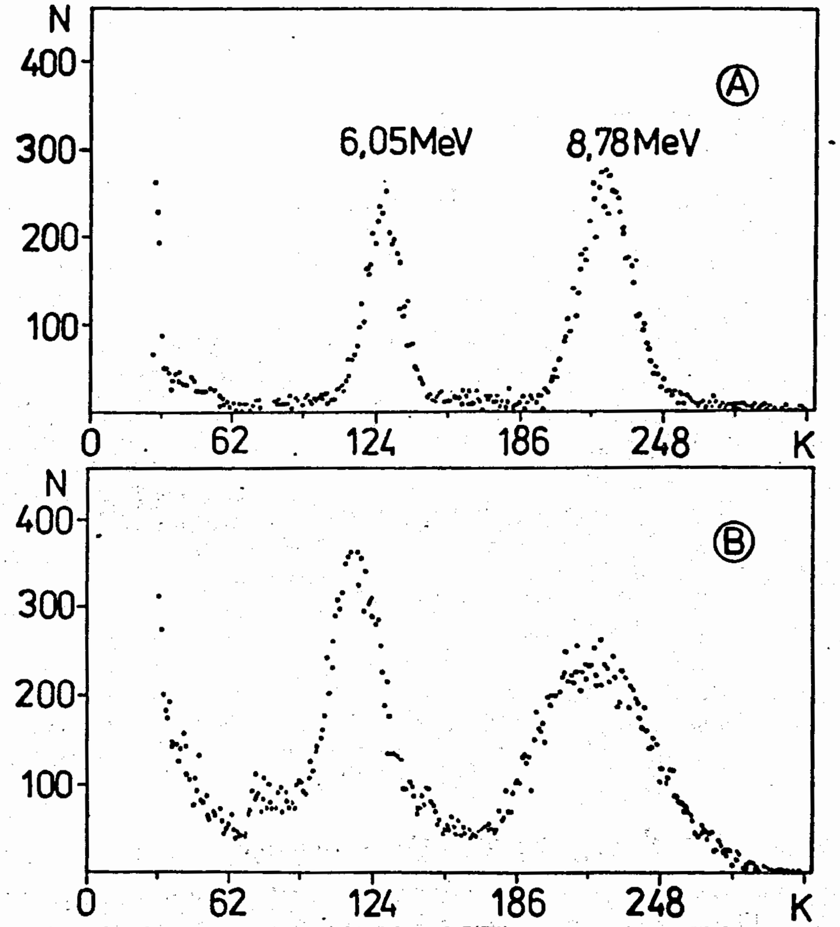

Fig. 5 Pulse-height spectra measured with a CsI(Tl) counter using a ThC-α-source. (A) for a collimated source irradiating only the central part of the scintillator. (B) for an uncollimated source, placed at 30 cm from the scintillator.

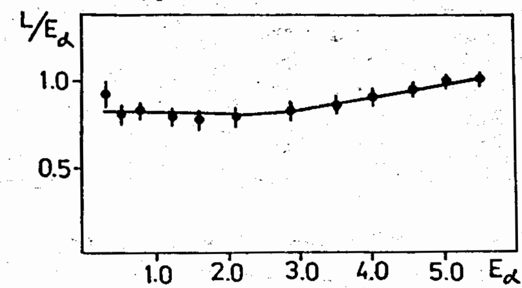

Fig. 6 The quantity L/E_α (light output over α energy) of a polycristalline CsI(Tl) film as a function of the α-particle energy.

30 cm away. The amplitude resolution was worse in comparison to that obtained with a collimated source. Only scintillators with $\Delta E/E$ better than 30% were selected for use in the FASA device.

3.4 Light output of a CsI(Tl) layer for fragments of different charge and energy.

Due to the quenching effect the scintillation efficiency does not depend linearly on the energy loss of a particle. To check whether the quenching in polycrystalline layers is the same as in monocrystalline CsI(Tl) [5] an experiment was performed using ^{4}He, ^{6}Li and ^{14}N beams accelerated by the Kurchatov Institute cyclotron. A carbon foil (0.5 mg/cm^2) was used as a target for the elastic scattering of the beam particles detected at an angle of 30^0 by a control sample of the CsI(Tl) scintillators. The recoiling nucleus was detected in coincidence by a telescope set at an angle, chosen by the kinematics for elastic scattering. The results are presented in fig. 7. The solid curves are calculated with the light-output of monocrystalline CsI(Tl) given in ref. [5]. Their results, obtained for ^{4}He, ^{12}C, ^{14}N and ^{16}O, have been fitted using polynomials of 4th order and the parameters have been interpolated for the other isotopes. The light output of the thin scintillator layers was calculated using a parametrized energy-loss formula [6], taking into account the selfabsorption of the scintillation light in the polycrystalline films. The results have been normalized to the experimental data points using the light output obtained for α particles from an ^{241}Am source. One can conclude that the dependence of the light output on the particle energy and charge is the same for mono- and polycrystalline CsI(Tl).

The results are used to calculate the efficiency of the scintillators for the detection of different fragments as a function of the energy. The light output of the CsI(Tl) foils has been assumed to be Gaussian distributed with a halfwidth of 30%. Figure 8 shows the efficiency curves calculated for a threshold of 2 times the pulse height of ^{241}Am α-particles. It illustrates the possibility of selecting fragments with $Z > 2$.

3.5 Background determination for the scintillation counters

The main beam coming into FASA is accompanied by a halo of fast secondary particles. These create Cherenkov radiation in the light guides providing very high counting rates in the low energy part of the pulse-height spectra and many chance coincidences. To reduce these chance coincidences a double-gate mode in the PM-pulse processing has been applied which works like a pulse-shape discrimination. The main gate (1.1 μs after the TOF trigger) serves to integrate the energy signal at its maximum while with the "early" gate (0.5 μs earlier) the rising part of the signal is selected in the case of true events. Double-gate plots for one of the PM's are shown in fig. 9, triggered by the E-counter and pulser alone (a) and requiring a E-ΔE coincidence of the TOF telescope (b). It clearly shows that all events can be divided into two parts: (i) the locus of the true events marked by the parallelogram-shaped window which was used for the off-line analysis and (ii) the chance coincidences.

With this procedure chance coincidences can be monitored during the runs and their contribution to the spectrum can be reduced significantly. The amount of chance coincidences inside the window of "good events" is determined to be 3-10% at 3.65 GeV/nucleon

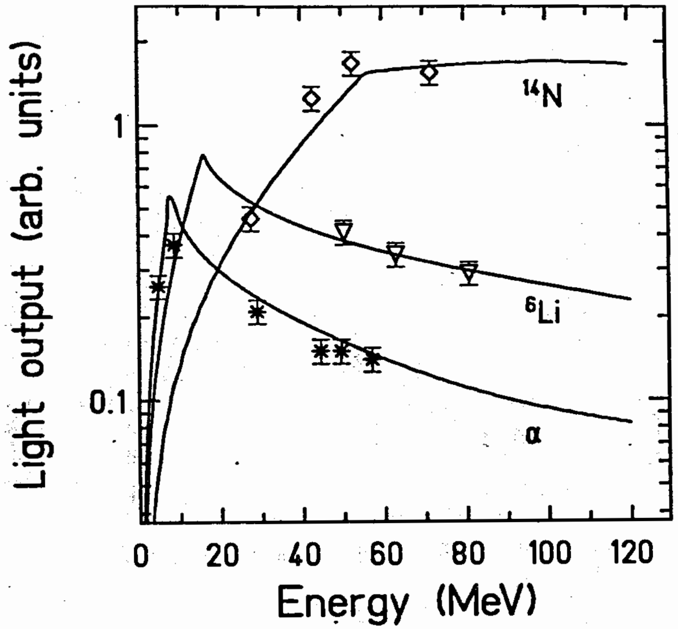

Fig. 7 The light output of a CsI(Tl)-layer as a function of the energy for α, ^{6}Li and ^{14}N particles. The solid curves are calculated using the light output for monocrystalline CsI as given in [5].

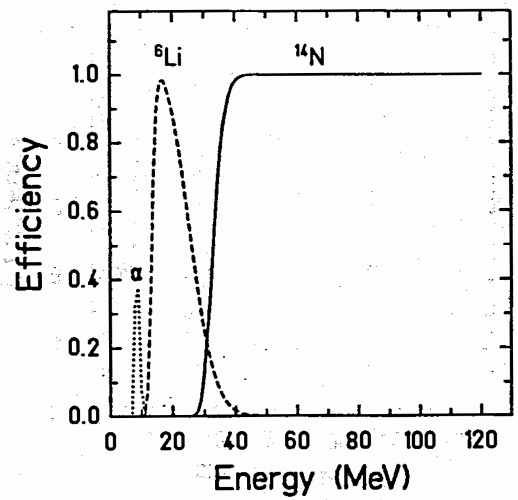

Fig. 8 The calculated efficiency of a CsI(Tl) counter for different particles as a function of their energy.

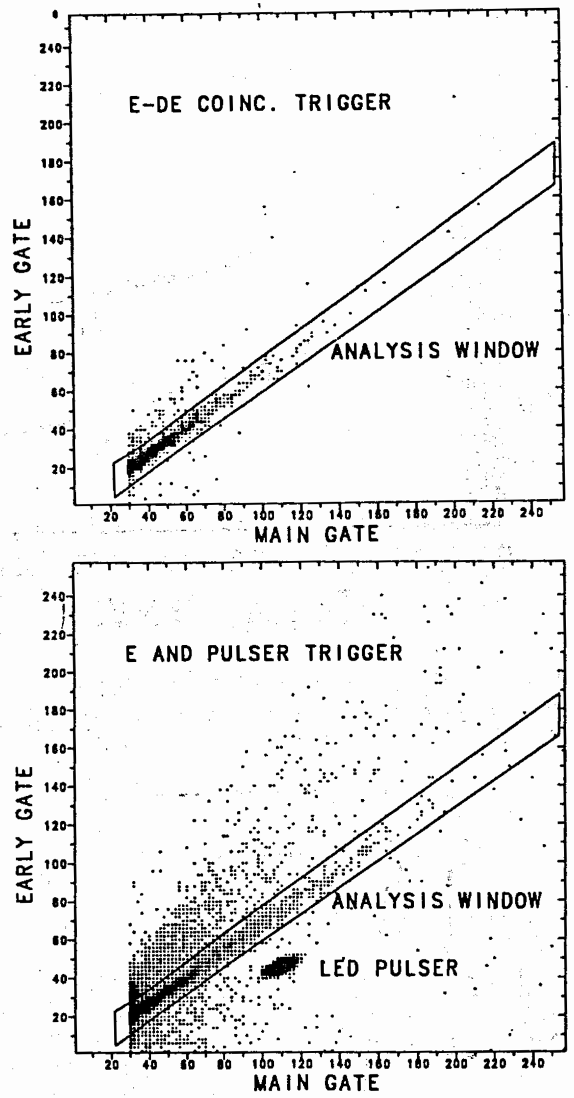

Fig. 9 Double-gate plots showing the separation of chance coincidences. The main gate is set at the maximum of the pulse while the early gate is placed on its rising part. The data were obtained by bombarding a Au target with α-particles of 3.65 GeV/nucleon. Lower part: triggered by the energy signal of the stop counter in the TOF telescopes and by the pulser. Upper part: triggered by ΔE-E coincidences of the TOFs.

α particles on ^{197}Au and with a beam intensity of $5 \cdot 10^8$ particles per spill, depending on the position of the scintillation counters.

4 Time-of-flight telescopes

The time-of-flight telescopes (TOF) are designed to be interchangeable with the CsI(Tl) scintillators. The TOFs' are used to obtain precise information on the measured fragments and to trigger the whole setup. Therefore, their design reflects a compromise between mass resolution (long flight path) and solid angle coverage (short path). Hence, detectors with a very good time resolution are chosen. A transparent parallel-plate avalanche detector (AC) at 25 cm distance from the target is used as the start counter. The particles are stopped in a surface barrier detector (SBD) placed 36 cm behind the AC. The solid angle of a TOF is $\Delta\Omega = 0.011$ sr which is defined by the SBD's diameter of 73 mm.

The start AC is designed to obtain large signal heights to optimize the signal-to-noise ratio for light particles. Therefore a high efficiency for the detection of IMF's is reached with the electronic thresholds chosen for the experiment. Very thin entrance foils are used to minimize the energy loss for heavy fragments. Figure 10 shows a cross-section of the counters. Two wire planes are placed symmetrically on each side of the central anode foil, yielding twice the amplitude of a single gap. The window foil consists of a 60 μg/cm^2 thick layer of Formvar supported by a Ni-mesh with 95% transmission. The central anode is a 40 μg/cm^2 thick Formvar foil, evaporated with Au on both sides. The wire planes consist of 50 μm thick, gold-plated tungsten wires with 1 mm spacing. The AC is operated with isobutene at 5 mbar and typically 630 V between the central electrode and the wire planes. Under these conditions a very high first Townsend coefficient of 47 cm^{-1} is reached. With the electronic threshold chosen for the experiment, efficiencies for α-particles from an ^{241}Am-source lie between 83% and 97% for the five TOFs' installed. Hence, the AC's do not imply any restriction on the detection of IMF's.

The stop counters are circular SBD's made out of n-Si with a specific resistivity of 450 Ωcm. The thickness is 500 μm and, operated at 150 V, a depletion depth of about 150 μm is reached. These characteristics have been chosen to obtain a good timing signal and to avoid a large pulse-height defect. The latter point has been studied extensively in an elastic-scattering experiment using different projectiles [7]. For nuclei up to Ni this effect is neglegible. Studies with J and Au beams show that the pulse-height defect is mainly due to nuclear stopping and only to a small extent to recombination.

The mass spectra are calibrated using a ^{252}Cf-source on a Ni-backing. For the mass calibration the energy-time information is used and the masses are calculated with an iterative procedure, which corrects for the the pulse-height defect [8] and the plasma delay [9]. Figure 11 displays the mass distribution of ^{252}Cf fission fragments, measured with a TOF telescope. A mass resolution of better than 10% is estimated from this spectrum which allows resolution of individual masses of light IMF's. Figure 12 demonstrates this ability, showing the mass distribution for the $4 \leq A \leq 12$ as measured in the experiment using α-projectiles of 3.65 GeV/nucleon on a Au target. From this spectrum a mass resolution of 8%, equivalent to a minimum time resolution of 400 pS, can be deduced for the TOF telescopes. It has to be noted that the spectrum shown in fig. 12 was collected during 4 days, evidencing the high stability of the counters and the electronics.

Due to the limited thickness of the SBD not all IMF with $Z \leq 4$ are stopped. They are

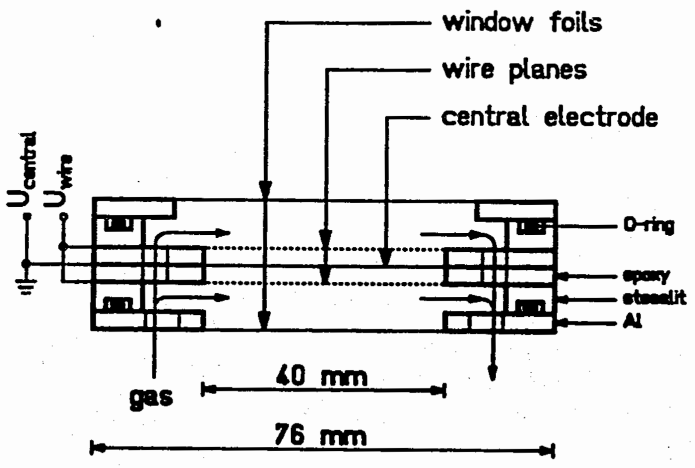

Fig. 10 Cross-section of the start AC.

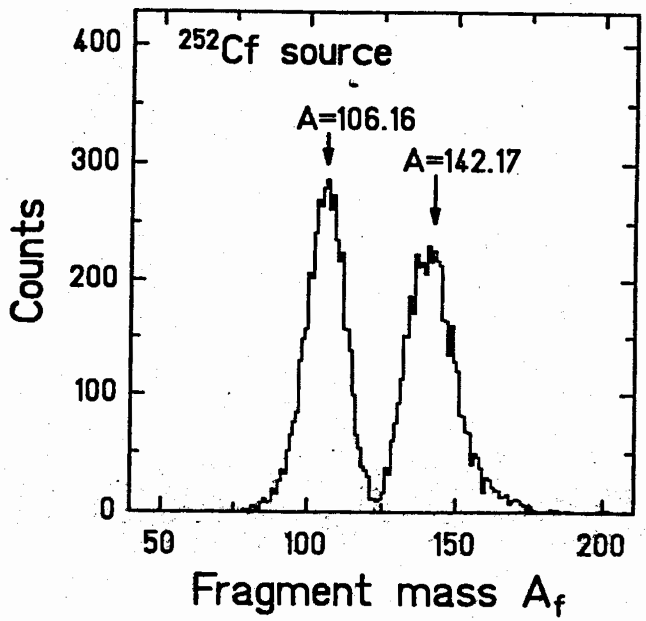

Fig. 11 Mass spectrum of fission fragments from a Cf-source measured with a TOF telescope. The energy and time-of-flight information of the telescope has been corrected for pulse-height defect and plasma delay.

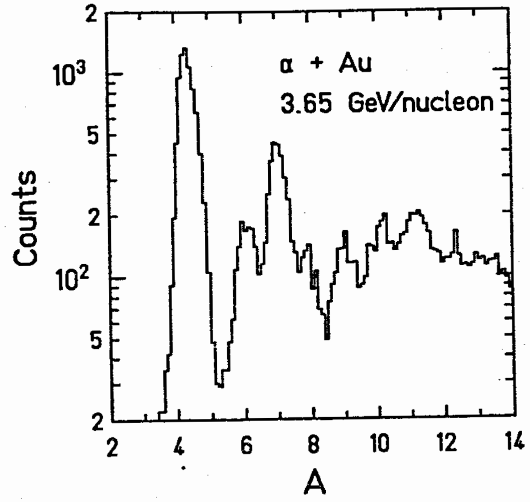

Fig. 12 Mass spectrum for fragments with $4 \leq A \leq 14$ for the reaction α on Au at 3.65 GeV/nucleon as measured with a TOF telescope.

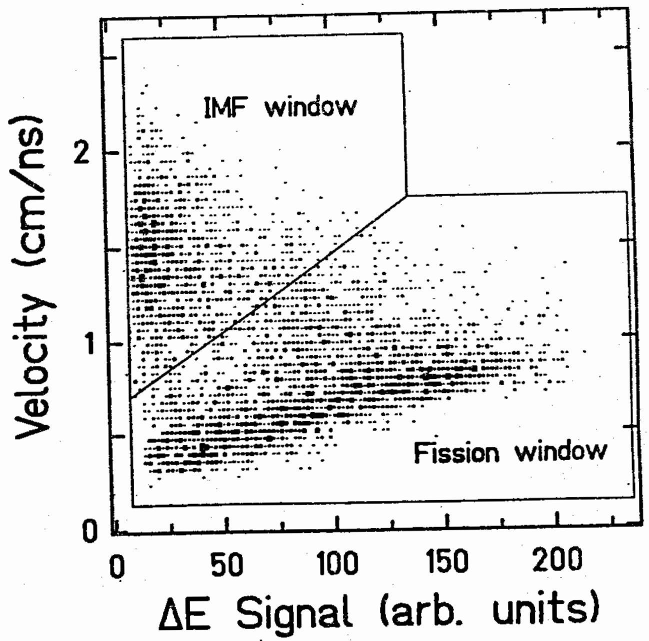

Fig. 13 Two-dimensional representation of the ΔE-signal versus the velocity of the fragment detected in the PPAC. Shown are the windows for selecting IMF and fission fragments in the off-line analysis.

identified in a two-dimensional representation of the time of flight versus the measured energy and are separated in the off-line analysis. The yield of fragments with $A \leq 10$ given in fig. 12 is decreased by this effect. The yield for the α particles is further reduced by the efficiency of the AC.

5 Position-sensitive parallel-plate avalanche counter

A position-sensitive PPAC [10] with an active area of 30×30 cm^2, is located 34 cm from the target at 63^0 to the beam axis. It is mounted opposite to three of the TOF telescopes giving large angle correlations and near to the two other telescopes yielding the small angle correlations. It is a transmission-type counter with a symmetric design. A cathode foil made from 1.5 μm Hostaphan covered on both sides with silver, is placed in the centre. At 3 mm distance on both sides, wire planes made of 20 μm thick, Au-covered tungsten wire with 1 mm spacing, form the x- and y-plane. Always four wires are grouped together and read out by a delay line with 2 ns per group. The read out is performed on both ends of the delay line which allows a recognition of multiple hits since then the sum of the two time delays does not add up to the total delay-line length. Using isobutene with a pressure of 3 mbar the cathode plane is operated at 530 V. The cathode delivers a time-stop signal and energy-loss information.

With the thresholds used in the experiment fragments with $Z > 5$ were detected with more than 90% probability.

The PPAC is read out only for coincidences with the TOFs' since only then can the velocity of the fragments in the PPAC be evaluated. In a two-dimensional representation of the energy-loss signal of the fragments detected by the PPAC versus the velocity, IMF and fission fragments can be separated. This is shown in fig. 13, which shows the ΔE - velocity distributions as obtained in the reaction α on Au at an energy of 3.65 GeV/nucleon.

6 Data acquisition electronics

The fast signal of the SBD is used as a trigger pulse, generating the gates for all the QDC's and ADC's of the system. It is also used as a start signal for a TDC that measures the time of flight in the TOF and the time of flight of the coincident fragment in the PPAC. As stop signals the delayed pulses from the ΔE-counters of the telescopes and the position-sensitive chamber are used. All fast pulses are converted into logic signals by constant-fraction discriminators. The time-to-digital converters have a bin width of 200 ps/ch.

The coordinates of a fragment passing through the PPAC are determined by a TDC that is started by the cathode signal of the chamber and stopped by the signals from the delay lines. Coincidences between the PPAC and the SBD are accepted during a gate time of 225 ns.

The data from the time and amplitude converters arrive at two buffers KL033 which are polled by a controller of the type KK009 [11] and then are fed into a PC AT386.

In the experiment the trigger rate was $\approx$ 150 per spill (spill length 300 mS), the electronic dead time was 15 %.

Acknowledgements

We would like to thank W. Patzner from the Institut für Kernphysik, Technische Hochschule Darmstadt for manufacturing excellent SBDs', A.F. Novgorodov for manufacturing and calibrating the α-source, J. Hutsch, U. Baumann and I. Probst from the Institute für Kern- und Hadronenphysik, Rossendorf for providing the very thin window foils and the grids for the small parallel-plate detectors and V.G. Sazonov for performing with skill the mechanical part of this setup. The authors are indebted to Profs. A.M. Baldin, E. Kankeleit and Ts. Vylov for their support of this work.

References

[1] Proceedings of the international conference on "New Physics with Advanced Techniques", Ieraptra, Greece, 1991, eds. F.A. Beck, S. Kossionides and C.A. Kalfas, (World Scientific, Singapore).

[2] M. Jääskeläinen, D.G. Sarantites, R. Woodward, F.A. Dilmanian, J.T. Hood, R. Jääskeläinen, D.C. Hensley, M.L. Halbert, and J.H. Barker, Nucl. Instrum. Meth. 204 (1983) 385.

[3] Y. Vidaj, Y.A. Tsirlin, and E.F. Tchaikowski, Izvestia AN USSR 38 (1974) p.1307.

[4] D. Dorczoman, D. Lazarevic, I. Muntyanu, K.O. Oganessian, and S.Y. Porohovoj, Pribori i technika experimenta 4 (1979) p.86.

[5] A. R. Quinton, C. E. Anderson, and W. J. Knox Phys. Rev. 115(1959)886.

[6] K. Braune, and D. Schwalm, GSI-J-1-77 (1977)

[7] R. Barth, diploma thesis, Technische Hochschule Darmstadt, 1992.

[8] S.B. Kaufman, E.P. Steinberg, B.D. Wilkins, J. Unik, A.J. Gorski, and M.J. Fluss, Nucl. Instr. Meth. 115 (1974) 74.

[9] H.O. Neidel, H. Henschel, N.Geissel, and Y. Laichter, Nucl. Instr. Meth. 212 (1983) 299.

[10] H. Stelzer, H. W. Daues, and N. Shenhav, GSI 85-1 (1985) 293.

[11] N.I. Zhuravlev, G. Kreipe, T. Opalek, A.P. Pavlov, V.T. Sidorov, A.N. Sinaev, A.A. Stahin, and I.N. Churin, JINR-Report P-10-88-937, Dubna, 1988.

Received by Publishing Department
on December 22, 1992.